View Article Online
DOI: 10.1039/C5AN00889A

Analyst

RSCPublishing

COMMUNICATION

Cite this: DOI: 10.1039/xoxxoooooox

Enhanced fluorescence detection of miRNA-16 on a photonic crystal

Received ooth January 2012,
Accepted ooth January 2012

DOI: 10.1039/xoxxoooooox

www.rsc.org/

F. Frascella[a], S. Ricciardi[a], L. Pasquardini[b], C. Potrich[b,c], A. Angelini[a], A. Chiadò[a], C. Pederzolli[b], N. De Leo[d], P. Rivolo[a], C.F. Pirri[a] and E. Descrovi[a]

We report on a novel sensing method for fluorescence-labelled microRNAs (miRNAs) spotted on an all-dielectric photonic structure. Such a photonic structure provides an enhanced excitation and a directional beaming of the emitted fluorescence, resulting in a significant improvement of the overall signal collected. As a result, the Limit of Detection (LoD) is demonstrated to decrease by a factor of about 50. A compact read-out system allows a wide-field imaging-based detection, with little or no optical alignment issues, which makes this approach particularly interesting for further development such as for example in microarray-type bioassays.

MicroRNAs (miRNAs) are small noncoding RNAs, acting as post-transcriptional regulators of gene expression in a broad range of species from algae to animals[1]. They have been widely studied over the past decades as promising biomarkers, for both diagnostic and therapeutic applications[2], because they could be over- or under-expressed in different pathological responses such as diabetes[3], neuro degenerative disorders[4] and various cancer[5].

Detecting miRNAs is one of the new challenges of analytical technologies. Unlike the classical protein biomarkers, miRNAs are characterized by short sequence lengths, which make the detection particularly difficult in terms of specificity. In an attempt to increase the specificity of the recognition while decreasing the minimum detectable amount of miRNA (Limit of Detection, LoD), several detection approaches have been proposed in the past. Basically, most of these strategies stems from conventional RNA analysis techniques, including amplification (e.g. reverse transcriptase polymerase chain reaction RT-PCR) and pre-concentration protocols (e.g. based on the use of carriers such as micro-beads and the like), that increase the overall amount of miRNA molecules at the detection stage[6-8]. However, new trends suggest to minimize the use of amplification steps because of several advantages, such as rapidity, ease of sample preparation and multiplexing capabilities[9,10]. Therefore, the very last detection step is required to be more and more sensitive[11-15].

Regardless of the strategies adopted for sample preparation, it is nevertheless beneficial to have sensing transduction means able to enhance the measured signal at the detection stage. Concerning optical sensors, and in particular those based on fluorescence, some approaches have been proposed to amplify the intensity of light emitted upon miRNA hybridization with a specific probe[16]. Plasmonic nanostructures have been widely investigated to this end[17], but an interesting alternative is represented by all-dielectric nanostructures called Photonic Crystals (PC)[18-21].

In this work, we demonstrate how a properly functionalized[22] all-dielectric structure is able to enhance the sensitivity in a fluorescence-based detection of labelled miRNA, resulting in a decrease of the LoD by a factor of about 50. The detection is performed as a wide-field imaging of the photonic structure surface, which can be advantageously exploited for highly parallelized micro-array type assays.

The detection is performed by means of a compact fluorescence microscope, as illustrated in Fig.1 (a).

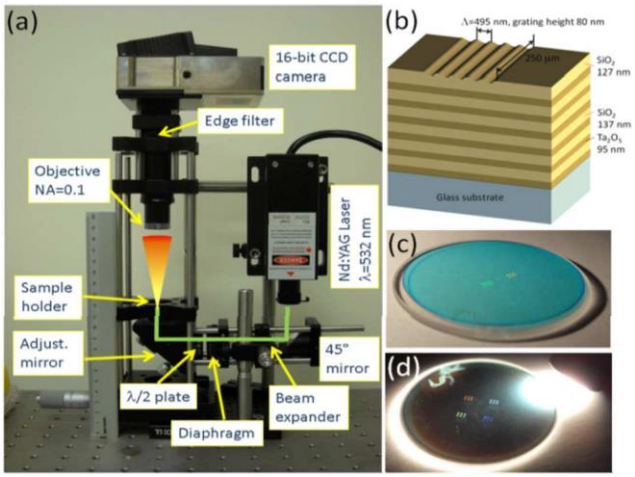

Fig.1 (a) Picture of the optical reading out system. A polarized, expanded laser beam illuminates the sample under an adjustable incidence angle, in such a way that a resonant illumination is reached. The enhanced fluorescence emitted from the sample is directionally beamed by the photonic structure toward the imaging optics; (b) sketch of multilayer with the periodic corrugation (coupling grating) on top; (c,d) pictures of a real chip, having 4 grating groups, with 6 gratings each. Colour effects are due to diffraction.

COMMUNICATION
View Article Online
DOI: 10.1039/C5AN00889A

The light source is a doubled frequency Nd:YAG laser beam (λ=532 nm), that is linearly polarised and collimated through a beam expander. The lateral size of the beam is limited by a diaphragm and the polarization rotated by a λ/2 plate. The laser beam is incident on the bottom side of the sample upon reflection on an adjustable dielectric mirror. In this way, the light incidence angle and polarization can be varied in order to match the resonance coupling condition of the photonic structure, as described later. The illumination spot covers a circular area 1 mm in diameter. The fluorescence emitted by the labelled species is collected by a Numerical Aperture, NA=0.1 lens and then imaged onto a 16-bit CCD camera after laser-filtering (Semrock RazorEdge MaxLine 532).

This optical readout system can hold a photonic chip (eventually capped with a polymeric fluidic circuitry)[23] based on a 1-inch diameter glass slide. The photonic structure consists of a periodically patterned dielectric multilayer (Fig.1 (b)). The multilayer, also called one-dimensional photonic crystal (1DPC), is a stack of 20 alternating layers made of a low and a high refractive index materials, (SiO_2 and Ta_2O_5, respectively) deposited by plasma ion assisted deposition under high vacuum conditions (APS904 coating system from Leybold Optics). Ta_2O_5 layers are 95 nm thick and SiO_2 layers are 137 nm thick, except for the last SiO_2 layer on top of the structure, which is only 127 nm thick. The 1DPC surface is patterned with 4 groups of 6 linear coupling gratings by means of Electron Beam Lithography. After a deposition of 80 nm of silica and the subsequent lift-off process, we obtained linear gratings with a height of 80 nm and a spatial period of Λ= 495 nm. Each grating is 250 μm x 250 μm in size. The overall appearance of the whole chip can be appreciated in Fig.1 (c,d).

The multilayer is designed and fabricated for sustaining s-polarized Bloch Surface Waves (BSW). BSW are surface modes that can be coupled at the truncation interface of photonic crystals of different dimensionalities,[24] including the planar and corrugated multilayers[25,26]. Thanks to the generally low loss of the underlying materials, BSW can propagate for long distances[27]. An interesting feature of BSW relies in the associated high near-field intensity that is produced very close to the truncation interface of the photonic crystal[28,29]. This effect is exploited to boost the fluorescence excitation of emitters located on the surface of the photonic crystal.[30]

In the present configuration, BSW are laser-coupled through the linear gratings, with no need of additional coupling prism in back-contact of the sample (the so-called Kretschmann configuration). Calculations[31] show that the present multilayer, patterned with a Λ=495 nm, can couple BSW having a rather intense near-field at the corrugation surface. Results are presented in Fig.2 (a), wherein the transverse laser intensity distribution across (and within) the corrugated multilayer is reported. More specifically, if a s-polarized λ=532 nm radiation illuminates the photonic structure from the bottom (glass) side, with an incidence angle of 1.6 deg, a resonant coupling to BSW is produced, resulting in an intense field confined at the truncation interface. Since the incidence angle is small, this illumination condition can be easily achieved by slightly tilting the adjustable 45 deg. mirror in our experimental apparatus. As a consequence, a maximum enhancement factor of roughly 30 is expected within few nanometers from the grating surface. Diffraction efficiency calculations show that the BSW resonance has a full angular width of about 0.5 deg., which is convenient for coupling from many low-cost laser sources. For example, a laser beam having a 1 mm transverse size and a 1 mrad divergence can produce a 10% variation of the surface field intensity if angularly offset by ±0.2 deg from the resonance angle. Laser beams with smaller divergence can provide illumination over larger areas without significantly decreasing the tolerance in the angular positioning of the illumination.

In addition to the BSW laser coupling, the grating on the multilayer produces an interesting directional beaming effect, described elsewhere[32,33]. Very briefly, when a fluorophore is located close to a properly patterned multilayer, it can transfer a significant amount of the radiated fluorescence to the BSW,[34] which gets suddenly diffracted by the corrugation. As a result, the angular distribution of the emitted radiation deviates from the conventionally isotropic distribution and becomes highly directional[35]. We calculated[33] the angular distributions of light emitted in air by a point-like source at λ=570 nm located either on the corrugated or on the flat multilayer. Results are presented in Fig.2 (b). The angular patterns are considered over a plane perpendicular to the corrugation grooves and the source dipole momentum, whereby the emitted radiation is substantially s-polarized.[30] On the air side, the beaming effect produced by the periodic corrugation is such that a pair of high-intensity peaks appears in an angular range within 11.5 degrees about the surface normal. This angular range corresponds to the acceptance angle of a collection optics having a 0.1 NA. By integrating the overall intensity collected under such an angular range, a gain of about 5 is found when comparing the collection from the grating and a flat area.

From the previous discussion, it appears that this kind of photonic structure is capable to provide (i) a fluorescence excitation enhancement on the surface by a theoretical factor of about 30 and (ii) a redirection of the emitted radiation resulting in an improvement in the collected fluorescence (NA=0.1) by a theoretical factor of about 5. The two effects being independent, they can be simultaneously exploited in such a way that an overall improvement of about 150 is expected in the detected fluorescence.

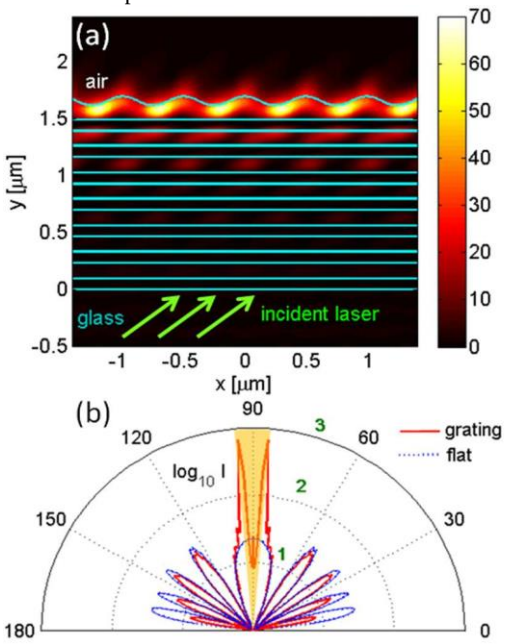

Fig.2 (a) Cross sectional distribution of s-polarized light through the patterned multilayer. Radiation comes from the glass substrate and is incident on the grating with an angle of 1.6 deg. whereby a BSW coupling condition is reached. A field enhancement of roughly 30 can be appreciated as produced close to the surface of the photonic crystal; (b) angular distribution of the radiation intensity (in a $\log_{10}$ scale) emitted in air by a point-like source located either on a flat multilayer (blue dotted line) or on a corrugated multilayer (red solid line). A directional beaming effect is observed wherein most of the radiated power is forward-emitted within an angular range of about 11.5 deg. (yellowish region).

Analyst View Article Online DOI: 10.1039/C5AN00889A COMMUNICATION

The effectiveness of the photonic crystal-assisted detection is demonstrated for miRNA-16 molecules labelled with AlexaFluor546 dye. The photonic crystal surface is functionalized via epoxy-chemistry (0.01% (3-Glycidoxypropyl) methyldiethoxysilane, 60°C, 10 min). Then, 100 µM amino-modified c-DNA strands are incubated in 0.5 M sodium phosphate buffer pH 7.3 for 3 hours at room temperature and therefore covalently bond, and used as miRNA probes. After a passivation step with 1 mM ethanolamine for 30 min and extensive washes, the photonic crystal is let drying in air. Different concentrations of labelled miRNA-16 are incubated in Nexterion hybridization buffer (SCHOTT AG, Germany) on the crystal for 1 hour at 48°C. After extensive washes in buffers with decreasing ionic strength (from SSC 2X plus 0.1% SDS, to SSC 2X, SSC 1X and finally ultrapure water), the crystal is imaged. In Fig.3 schematic of the surface functionalization is shown.

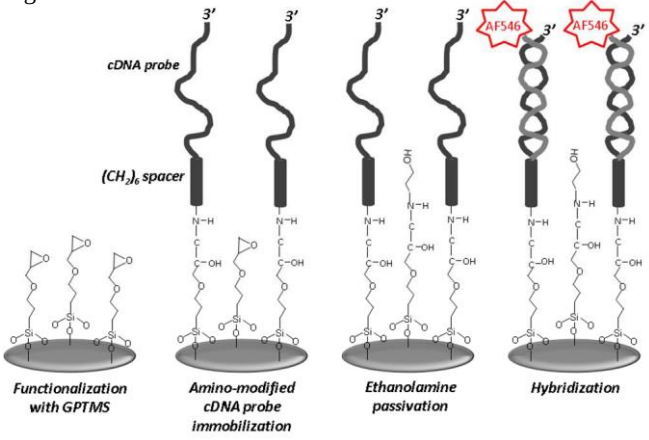

Fig.3 Sketch illustrating the surface functionalization and detection protocol for miRNA-16 recognition.

We implemented a detection approach whereby groups of gratings can be simultaneously illuminated and imaged onto the 16-bit CCD. In Fig.4 an exemplary fluorescence image (rendered in false-colours) is shown involving a group of 4 gratings upon binding of miRNA-16 at a concentration of 50 nM.

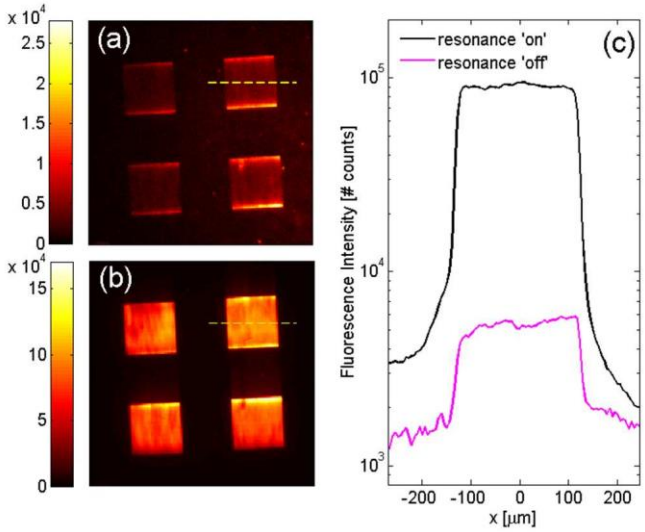

Fig.4 Fluorescence image (in false colors) of a sub-group of 4 gratings either non-resonantly (a) or resonantly (b) excited by the incident laser beam (incidence is 1.6 deg) upon polarization rotation; (c) comparison of intensity profiles across one grating (yellow dashed line in (a,b)) in on-resonance and off-resonance conditions.

Fluorescence can be excited either non-resonantly or resonantly by simply rotating the polarization of the incident laser by 90 degrees. When the polarization is perpendicular to the grating grooves, the illumination is off-resonance and the fluorescence excitation enhancement is switched off (Fig.4 (a)). On the contrary, when the polarization of the laser is parallel to the grating grooves, BSW can be coupled and the illumination gets resonant (Fig.4 (b)). It is interesting to consider the fluorescence intensity cross-section (after dark current subtraction) across the gratings in the off-resonance and on-resonance conditions (Fig.4 (c)). In the former case, the intensity profile is not constant, the fluorescence being about three times higher on the gratings as compared to the flat surroundings (magenta line in Fig.4 (b)). The observed increase is due to the directional beaming effect acting on the fluorescence that is non-resonantly excited by the laser. In the latter case, the fluorescence coming from the gratings is further increased by a factor of about 20, the resonant excitation producing an overall enhancement of about 60 as compared to the flat surroundings (black line in Fig.4 (b)). Experimental observations are below the theoretical predictions reported above, probably because of fabrication tolerances.

The simplicity of operation of the proposed detection system allows us to build up a titration curve for miRNA-16 over a rather large concentration range. We consider miRNA-16 concentrations ranging from 0.5 nM to 2.5 µM, wherein each concentration has been incubated on a single group of 6 gratings. Fluorescence intensity values are extracted from either the grating regions or the flat regions surrounding the gratings by means of an automatic off-line image processing algorithm, calculating intensity averages over defined areas, after dark-current subtraction. All values are then plotted in the titration curve shown in Fig.5. The error bars take into account the fluorescence fluctuations over the 6 gratings with miRNA-16 incubated at identical concentrations.

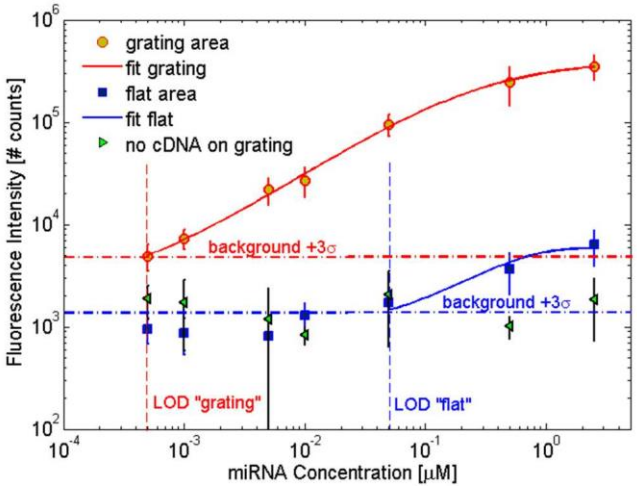

Fig.5 Fluorescence titration curve collected for different miRNA-16 concentrations, inside and outside the gratings. The reported concentration refers to the miRNA-16 molarity in the incubating solution.

In a double logarithmic scale, both curves are well fitted by a sigmoidal profile,[36] with the low-concentration values asymptotically approaching the background level. The background fluorescence has been estimated by considering the mean fluorescence intensity from the sample surface before miRNA-16 incubation, with only c-DNA probes grafted. Since the enhancement effects due to the photonic structure affect the background fluorescence as well, two different background levels have to be considered for either the gratings or the flat regions, respectively.

View Article Online
DOI: 10.1039/C5AN00889A

The background level is then determined with an associated uncertainty (the root mean square σ), therefore the minimum detectable amount of fluorescence from labelled miRNA-16 is defined by the background level increased by 3σ.

We can note that miRNA-16 at concentrations below 50 nM cannot be well discriminated from the background on the flat regions, whilst concentrations as low as 0.5 nM are still detectable on the gratings. For concentrations larger than 50 nM, the fluorescence enhancement factor is maintained within a range from 50 to 70. As a result, we have experimentally demonstrated that the Limit of Detection (LoD) is decreased by at least a factor of 50 in concentration. Non-specific binding due to interaction with the substrate results in fluorescence signals about the background level, as indicated by the flat dose response curve (green triangular marker).

Conclusions

In this work we presented an optical detection method fruitfully used for labelled miRNA in a micro-array fashion. More specifically, we developed a compact and portable optical read-out system hosting a photonic-crystal chip where analyte species are incubated thereon. Thanks to BSW-mediated coupling and diffraction effects it is possible to obtain wide-field images of the chip surface with enhanced fluorescence intensity. Contrary to other approaches based on planar multilayer for fluorescence enhancement[30,37], the grating allows a direct transfer of energy from/to free-space radiation to the surface mode sustained by the photonic crystal.

The method is demonstrated for synthetic miRNA-16 Alexa Fluor 546 labelled in buffer, leading to a significant decrease of the Limit of Detection. The implementation of un-labelled microRNA detection is also possible with different strategies, e.g. by using molecular beacon-like probes, labelling of target sequence or even competitive assay.

Because of the simplicity of use of the overall apparatus, this approach can be eventually up-scaled to large-area microarrays, wherein a plurality of different spots-on-grating can be simultaneously imaged onto a CCD camera.

Acknowledgements

This research has received funding from Italian FIRB 2011 NEWTON (RBAP11BYNP). The authors thank dr. Peter Munzert (IOF-Fraunhofer, Jena, Germany) for the multilayer deposition and dr. Luca Boarino (INRiM, Torino, Italy) for the EBL fabrication performed at Nanofacility Piemonte INRIM, a laboratory supported by Compagnia di San Paolo Foundation.

Notes and references

[a] Dipartimento di Scienza Applicata e Tecnologia, Politecnico di Torino, C.so Duca degli Abruzzi 24, 10129 Torino, Italy.
[b] Fondazione Bruno Kessler, Via Sommarive 18, 38123 Povo (TN), Italy.
[c] CNR-Istituto di Biofisica, Via alla Cascata 56/c, 38123 Povo (TN), Italy.
[d] Nanofacility Piemonte, Istituto Nazionale di Ricerca Metrologica, Strada delle Cacce 91, 10135 Torino, Italy.

† Electronic Supplementary Information (ESI) available: [details of any supplementary information available should be included here]. See DOI: 10.1039/c000000x/

1 H. Dong, J. Lei, L.Ding., Y. Wen, H. Ju and X. Zhang, *Chem. Rev.*, 2013, **113**, 6207.
2 B. N. Johnson and R. Mutharasan, *Analyst*, 2014, **139**, 1576.
3 M. N. Poy, L. Eliasson, J. Krutzfeld, S. Kuwajima, X. Ma, P. E. Macdonald, S. Pfeffer, T. Tuschl, N. Rajewsky, P. Rorsman and M. Stoffel, *Nature*, 2004, **432**, 226.
4 M. S. Nicoloso, R. Spizzo, M. Shimizu, S. Rossi and G. A. Calin, *Nat. Rev. Cancer*, 2009, **9**, 293.
5 N. Meola, V. A. Gennarino and S. Banfi, *Pathogenetics* 2009, **2**, 7.
6 J. Nelson, *Nat Methods*, 2004, **1**, 155
7 J.Q. Yin, *Trends Biotechnol*, 2008, **26**, 70.
8 J. Lu , G. Getz, E. A. Miska, E. Alvarez-Saavedra, J. Lamb, D. Peck, A. Sweet-Cordero, B. L. Ebert, R. H. Mak, A. A. Ferrando, J. R. Downing, T. Jacks, H. R. Horvitz and T. R. Golub TR, *Nature*, 2005, **435**, 834.
9 H. Sipova, S. Zhang, A. M. Dudley, D. Galas, K. Wang and J. Homola, *Anal. Chem.*, 2010, **82**, 10110.
10 A. J. Qavi, J. T. Kindt, M. A. Gleeson and R. C. Bailey, *Anal. Chem.*, 2011, **83**, 5949.
11 Z. Wang, J. Zhang, Y. Guo, X. Wu, W. Yang, L. Xu, J. Chen, F. Fu, *Biosens. Bioelec.*, 2013, **45**, 108.
12 R., Yuqian, D. Huimin, S. Wei, and Z. Gao, *Anal. Chem*., 2013, **85**, 4784.
13 B.N. Johnson and R. Mutharasan, *Anal. Chem*., 2012, **84**, 10426.
14 N. E. Larkey, C. K. Almlie, V. Tran, M. Egan, and S. M. Burrows *Ana.l Chem,*. 2014 **86**, 1853.
15 H. Šípová, S. Zhang, A. M. Dudley, D. Galas, K. Wang, and J. Homola, *Anal. Chem.*, 2010, **82** , 10110.
16 J. Y. Liao, J. Q. Yin and J. C. Yue, *Sensors*, 2009, 671896.
17 K. Ray, M. H. Chowdhury, J. Zhang, Y. Fu, H. Szmacinski, K. Nowaczyk and J. R. Lakowicz, *Adv. Biochem Eng Biotechnol*, 2009, **116**, 29.
18 N. Ganesh, W. Zhang, P.C. Mathias and B.T. Cunningham, *Nat. Nanotech.*, 2007, **2**, 515.
19 N. Ganesh, I.D. Block, P.C. Mathias, W. Zhang, E. Chow, V. Malyarchuk, and B.T. Cunningham, *Opt. Express*, 2008, **16**, 21626.
20 B. T. Cunningham, *Jala*, 2010, **4**, 120.
21 S. George, V. Chaudhery, Y. Tan, M. Lu, and B.T. Cunningham, *Lab on Chip*, 2013, **13**, 4053.
22 C. Pastells, M. Pilar, D. Merino, P. Loza-Alvarez, L. Pasquardini, C. Pederzolli, D. Farnesi, S. Berneschi, G. C. Righini, G. Nunzi Conti, S. Soria, *Proc. SPIE 9343*, 2015.
23 S. Ricciardi, F. Frascella, A. Angelini, A. Lamberti, P. Munzert,, L. Boarino, R. Rizzo, A. Tommasi and E. Descrovi, *Sens. Act. B*, 2015, **215**, 225.
24 K. Ishizaki and S. Noda, *Nature*, 2009, **460**, 367.
25 P. Yeh, A. Yariv and C. S. Hong, *J. Opt. Soc. Am.*, 1997, **67**, 423.
26 E. Descrovi, F. Giorgis, L. Dominici, and F. Michelotti, *Opt. Lett.*, 2008, **33**, 243.
27 E. Descrovi, T. Sfez, M. Quaglio, D. Brunazzo, L. Dominici, F. Michelotti, H. P. Herzig, O. J. F. Martin, and F. Giorgis, *Nano Lett.*, 2010, **10**, 2087.
28 I. Soboleva, E. Descrovi, F. Giorgis, C. Summonte and A. Fedyanin, *Appl. Phys. Lett*, 2009, **94**, 231122.

View Article Online
DOI: 10.1039/C5AN00889A

29 S. Pirotta, X. Xu, A. Delfan, S. Mysore, S. Maiti, G. Dacarro, M. Patrini, M. Galli, G. Guizzetti, D. Bajoni, J. E. Sipe, G. Walker and M. Liscidini, *J. Phys. Chem. C*, 2013, **117**, 6821.

30 R. Badugu, K. Nowazcyk, E. Descrovi and J. R. Lakowicz, *Anal. Biochem.*, 2013, **442**, 83.

31 L. Li, G. Granet, J.P. Plumey, and J. Chandezon, *Pure Appl. Opt.*, 1996, **5**, 141.

32 A. Angelini, E. Enrico, N. De Leo, P. Munzert , L. Boarino, F. Michelotti, F. Giorgis and E. Descrovi, *New J. Phys.*, 2013, **15**, 073002-1.

33 A. Angelini, E. Barakat, P. Munzert, L. Boarino, N. DeLeo, E. Enrico , F. Giorgis, H. P. Herzig, C. F. Pirri and E. Descrovi, *Sci.Rep*., 2014, **4**, 5428.

34 M. Ballarini, F. Frascella, F. Michelotti, G. Digregorio, P. Rivolo, V. Paeder, V. Musi, F. Giorgis and E. Descrovi, *Appl. Phys. Lett.*, 2011, **99**, 043302-1

35 A. Angelini, P. Munzert, E. Enrico, N. De Leo, L. Scaltrito, L. Boarino, F. Giorgis and E. Descrovi, *ACS Photonics*, 2014, **1**, 612.

36 B. T. Cunningham and R. C. Zangar, *J. Biophotonics*, 2012, **5**, 617.

37 R. Badugu, E. Descrovi, and J.R. Lakowicz, *Anal. Biochem*., 2014 **445**, 1.